

# Enabling data-driven and bidirectional model development in Verilog-A for photonic devices

DIAS AZHIGULOV<sup>1,\*</sup>, ZEQUIN LU<sup>2</sup>, JAMES POND<sup>2</sup>, LUKAS CHROSTOWSKI<sup>1</sup>, AND SUDIP SHEKHAR<sup>1</sup>

<sup>1</sup>*Department of Electrical and Computer Engineering, University of British Columbia, 2332 Main Mall, Vancouver, BC V6T 1Z4, Canada*

<sup>2</sup>*Ansys Lumerical Inc., 1095 W Pender St #1700, Vancouver, BC V6E 2M6, Canada*

\**dias.azhigulov@ece.ubc.ca*

**Abstract:** We present a method to model photonic components in Verilog-A by introducing bidirectional signaling through a single port. To achieve this, the concept of power waves and scattering parameters from electromagnetism are employed. As a consequence, one can simultaneously transmit forward and backward propagating waves on a single wire while also capturing realistic, measurement-backed response of photonic components in Verilog-A. We demonstrate examples to show the efficacy of the proposed technique in accounting for critical effects in photonic integrated circuits such as Fabry-Perot cavity resonance, reflections to lasers, etc. Our solution makes electronic-photonic co-simulation more intuitive and accurate.

## 1. Introduction

Photonic Integrated Circuits (PICs) play a critical role in many modern applications, ranging from communication to sensing [1]. The rise of CMOS compatible silicon photonic processes accelerated this trend. Practically, in each case, they are accompanied by electronics, either monolithically integrated into a single chip or otherwise. This necessitates a common simulation platform where one can simulate PICs and Electronic Integrated Circuits (EICs) to capture their interactions.

The co-simulation of EIC and PIC can be broadly categorized into two groups: Electronic Photonic Design Automation (EPDA) simulation and Electronic Design Automation (EDA) simulation. An example of the former is the Cadence-Lumerical EPDA platform [2] that conjoins two different simulators by exchanging simulation data back and forth between the two. It provides an accurate and versatile co-simulation platform, but transient simulations for circuits incorporating feedback can be slow. The EDA-only co-simulation leverages hardware description languages (HDLs) such as Verilog-A for compact modeling of photonic devices to support PICs natively in SPICE-class circuit simulators [3–8]. Since the number of electronic devices far exceeds their photonic counterparts in any silicon photonic application [1], Verilog-A-based native simulations bring ease and simplicity to system architects and CMOS designers. Kononov et al. [3] laid the groundwork for photonic component modeling, capturing effects such as phase shift, delay, attenuation, and electrical bandwidth. The follow-up works [4, 5] further improved the models and introduced new features such as multi-wavelength communication using a single wire and laser phase noise. They also presented complex system-level EIC and PIC co-simulation setups.

Silicon photonics integrated circuits operate at a carrier frequency of 100s of THz, and therefore must be treated as transmission lines. Therefore, capturing the impact of reflections is crucial for various circuits. For example, back-reflections from a PIC into a laser without an isolator can degrade the laser performance, and even destabilize it [9, 10]. Circuit techniques to stabilize the lasers [10–13] or improve its linewidth using self-injection locking [14] must capture reflections. Cavity-based optical filters [15] must account for reflection for accurate modeling of the filter frequency response.

The modeling of reflections and bidirectional signaling in Verilog-A has remained incomplete,

even leading to claims in [15] that Verilog-A-based co-simulation is not meant to handle such features. Nevertheless, several attempts have been made to address bidirectional signal propagation. Several models [4–7] handle the forward and backward propagating waves in separate wires. However, they do not account for reflections from all ports (e.g. in directional couplers). Additionally, reflection-centered devices such as Bragg gratings are not trivial to implement in Verilog-A. The previous methods are limited to what they can model since they all base it on analytical equations. This leads to simplifications in modeling and idealistic simulations.

Recently, de Foucauld et al. [8] presented a technique to handle reflections in the same wire as the transmitted signal without the two corrupting each other. The presented test bench is, however, very simple and not representative of more intricate photonic circuits. The authors state that their method does not hold up for the cases where multiple optical sources are present.

We present a methodology to capture forward and backward propagating signals using the same wire, without putting any limitations on all prior modeling techniques [16]. Through this work, one only needs to use half as many wires as being used in traditional Verilog-A photonic models. Moreover, by taking advantage of the bidirectional signaling technique we build measurement data-driven models for passive photonic devices using scattering parameters (*s-parameters*) [17]. Unlike the previous methods [4–7], this lets users recreate response of any arbitrary passive photonic element in Verilog-A without the need for device physics expertise that is required for conventional approach. This technique naturally captures fabrication induced imperfections as well. We highlight all the differences between this work and the prior arts in Table 1.

The paper consists of four sections. Section II describes the methodology of bidirectional signaling in Verilog-A with a brief theoretical background. In section III we simulate and present the results of circuits consisting of Verilog-A components to prove the viability of our solution. Section IV concludes our work.

Table 1. Comparison between this work’s features and prior arts.

	[4]	[8]	This work
<b>Model types</b>	Analytical & curve-fit	Analytical & curve-fit	Analytical, curve-fit, and measurement data based
<b>Bidirectional signaling</b>	2 ports	1 port	1 port
<b>Reflections</b>	No	Yes	Yes, from all ports
<b>Fabrication effects</b>	No	No	Yes
<b>Supports multiple optical sources</b>	Yes	No	Yes

## 2. Methodology

### 2.1. Theory

Before delving into the details of our implementation, it should be emphasized that at the baseline one can use the established techniques [3, 5] of photonic component modeling in Verilog-A. Our bidirectional signaling methodology simply encapsulates the behavioural description code of a device.

There is a large body of literature on analytical description of forward and backward propagating waves in electromagnetics theory [17]. One very pertinent concept to our problem is *power waves* and they are defined as:

$$a = \frac{V + Z_R I}{2\sqrt{R_R}} \quad (1)$$

$$b = \frac{V - Z_R^* I}{2\sqrt{R_R}}, \quad (2)$$

where  $a$  and  $b$  are forward and backward propagating wave amplitudes, respectively,  $V$  and  $I$  are the voltage and current present in a circuit.  $Z_R = R_R + jX_R$  is the reference impedance with resistance of  $R_R$  and reactance of  $X_R$ . For simplicity, we can assume that our reference impedance is purely real,  $Z_R = R_R$ , and its value can be arbitrary. Solving for  $V$  and  $I$  in Eq. 1 and 2 we get:

$$V = \frac{Z_R^* a + Z_R b}{\sqrt{R_R}} = \sqrt{R_R}(a + b) \quad (3)$$

$$I = \frac{a - b}{\sqrt{R_R}} \quad (4)$$

## 2.2. Implementation

Next, we explain how to incorporate the power waves into Verilog-A. Consider the basic example of a photonic circuit and its electrical counterpart shown in Fig. 1a and 1b. The former consists of the laser, photodetector, and a couple of black box elements, which may perform arbitrary functions on the input signals. In the latter, however, we describe every circuit element using its interfaces, that is, ports. Each port is a voltage source in series with a resistance (or more generally, an impedance). The sources can supply arbitrary voltages depending on the component behavior. In combination with the resistors, they allow current and voltage flow in the circuit thereby making bidirectional signaling possible. While various resistance values can be chosen to mitigate potential convergence issues, the key here is to set all of them to the same value  $R_R$ . It is important to set all the resistors to the same value  $R_R$ .

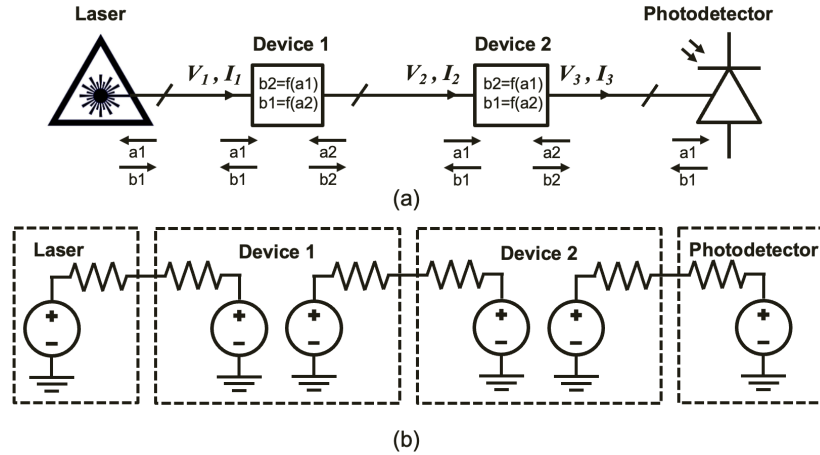


Fig. 1. (a) Illustration of a photonic circuit, (b) its electronic equivalent in Verilog-A.

To implement the bidirectionality in Verilog-A, one has to use the bidirectional ports (*inout* construct) in Verilog-A when defining all the optical ports. Afterwards, for any component, one can calculate the incoming wave amplitude at a given port using the voltage and current readings at that port and plugging them into Eq. 1. Then, the outgoing wave can be set as a function of

the incoming wave ( $b = f(a)$ ). There are no restrictions, besides the ones imposed by Verilog-A itself, on what kind of function this is. Following this, we compute either the new voltage or current values at each port through Eq. 3-4. In the context of the photonic circuit depicted in Fig. 1a, it can be noticed that there are forward and backward propagating waves at each port of a given device. Additionally, the voltage and current values vary from one node to another. Thus, while voltages and currents carry the information, the wave values  $a$  and  $b$  are the ones that represent the actual optical field. Such freedom in functionality and independence from node to node can occasionally lead to convergence issues due to widely varying currents and voltages throughout the circuit. If that is the case, controlling the signal's tolerance levels in Verilog-A can help alleviate the problem [18].

It should also be highlighted that for transmission lines, reflection takes place whenever there is a mismatch in impedance between two mediums (e.g. characteristic impedance of transmission line  $\neq$  load impedance). For power waves, reflection occurs when the reference impedance is not the same as the load impedance [17]:

$$\Gamma_p = \frac{b}{a} = \frac{V - Z_R^* I}{V + Z_R I} = \frac{Z_L - Z_R^*}{Z_L + Z_R}, \quad (5)$$

where  $\Gamma_p$  is the reflection coefficient of the power waves. In our Verilog-A models, we set  $Z_L$  and  $Z_R$  to the same real value. In this way, there are no reflections by default. The only source of reflections are the intermediate black box components.

To incorporate reflections into the black box models in Fig. 1, one can use analytical descriptions of the plane wave transmission and reflection off an interface [8] or one can utilize scattering matrices as an extension of the power waves concept [17]. The former has already been done in Verilog-A in [8]. We will only explore the latter approach due to its additional merits. Scattering matrix consists of s-parameters, which describe the response of linear electrical or optical networks at the port  $i$  to a certain input signal at the port  $j$  [19]. For a two port network/device it can be expressed as:

$$S = \begin{bmatrix} s_{11} & s_{12} \\ s_{21} & s_{22} \end{bmatrix} \quad \text{and} \quad s_{ij} = \frac{b_i}{a_j}, \quad (6)$$

where  $b_i$  is the outgoing wave at the port  $i$  and  $a_j$  is the incoming wave at the port  $j$ . The introduction of s-parameters is also advantageous for data-driven model development since all the devices can be characterized by the frequency dependent s-parameter data. In Verilog-A, one can import s-parameters as a Lookup Table (LUT) and write the equations for the outgoing waves using the s-parameters. For a generic  $n$ -port network this can mathematically be described as:

$$\begin{bmatrix} b_1 \\ \vdots \\ b_n \end{bmatrix} = \begin{bmatrix} s_{11} & \cdots & s_{1n} \\ \vdots & \ddots & \vdots \\ s_{n1} & \cdots & s_{nn} \end{bmatrix} \begin{bmatrix} a_1 \\ \vdots \\ a_n \end{bmatrix} \quad (7)$$

Thus, the outgoing waves for the two port devices from Fig. 1 are expressed as  $b_1 = s_{11}a_1 + s_{12}a_2$  and  $b_2 = s_{21}a_1 + s_{22}a_2$ . From the definition of s-parameters, it can be deduced that  $s_{11}$  is the reflection coefficient at port 1 and  $s_{21}$  is the transmission coefficient. Consequently,  $b_1$  now captures the transmitted signal from the opposite end as well as the reflected signal from the same port, giving rise to forward and backward propagating waves in our circuit. It should be emphasized that not every photonic device needs the s-parameter based model description (e.g. a homogeneous medium such as ideal waveguides does not produce any reflections). Using Eq. 1-4 is enough to run bidirectional simulations in any commercial EDA software. Finally, other equivalent representations such as T-matrix can also be used [17].

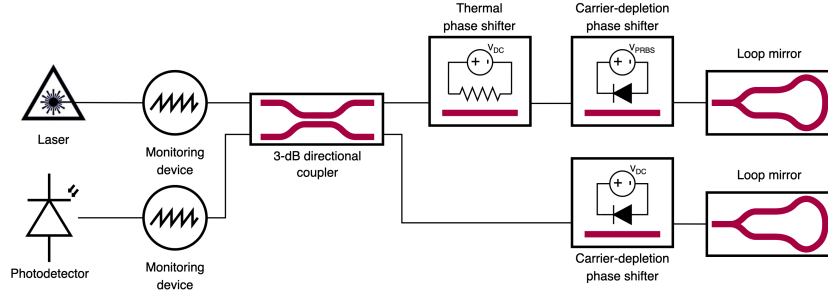


Fig. 2. Schematic diagram of the MIM built using Verilog-A components.

We note that all the commercial EDA tools already handle reflections when simulating electronic devices with transmission lines. The only caveat is that those tools keep everything in voltage and current domains. Thus, in order to observe reflections one has to interpret the voltage and current waveforms, which come as a superposition of transmitted and reflected signals. Since our situation is similar, we implement a monitoring device to read the optical power and phase of forward and backward propagating signals in a given node.

### 3. Simulation

To demonstrate the efficacy of our modeling approach, we built a Michelson Interferometer Modulator (MIM) using a Verilog-A library of silicon photonic devices [3, 5]. Most passive photonic device models in the library are built using the data from [20]. Active devices are developed through a combination of analytical description and simulation/measurement data [21, 22]. Laser is the only device in our library that has purely behavioural description because we use it as a continuous wave (CW) supply to the PICs. A MIM is an ideal testbench for demonstration of bidirectional signaling since the forward and backward propagating signals are simultaneously present in each arm. Furthermore, signals in both arm should constructively interfere to be able to see the modulated signal at the photodetector side. In case of destructive interference, all of the returning signals should appear at the laser side. In contrast to the example from [8], our testbench can be viewed to have three optical sources (one forward propagating signal from the laser and two reflected signals from the mirror loop) all meeting at the directional coupler. Thus, it does not have the limitation of the prior work.

Fig. 2 depicts the schematic view of the MIM assembled in Cadence Virtuoso. As per the typical MIM design, it consists of 3-dB directional coupler, thermal phase shifter, carrier depletion phase shifter, and loop mirrors built from Y-branch and waveguide bends. Note that the laser is internally set to have an isolator in order to keep feeding constant power, though this can be modified in the code. Fig. 3 shows the transfer function of the MIM with the output being seen at the laser and photodetector interfaces. We sweep the thermal phase shifter's bias voltage ( $V_{th}$ ) to produce this plot and record the backward propagating waves at the laser and photodetector ports. It is clear that the wave powers are complementary, which is to be expected. The transient behavior of the circuit is provided in Fig. 4. The reflected signals arrive at the laser and photodetector interfaces in accordance to the modulation signal. Furthermore, as expected, the laser's output signal (i.e. forward propagating signal) remains the same regardless of the incoming signals. Similarly, the photodetector's forward propagating signal is zero at all times.

We also built a testbench for the Bragg gratings based Fabry-Perot Cavity (FPC) simulation, similar to what is presented in [15], wherein the Verilog-A photonic models were deemed incapable of simulating bidirectional signal propagation. Figure 5 illustrates the developed testbench, where we design the FPC to have a resonant peak at the wavelength close to 1549 nm.

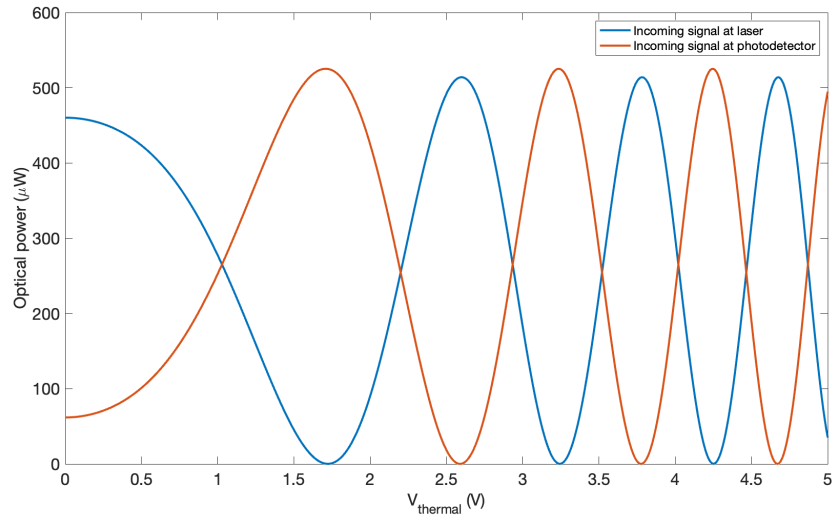


Fig. 3. Transfer function of the MIM.

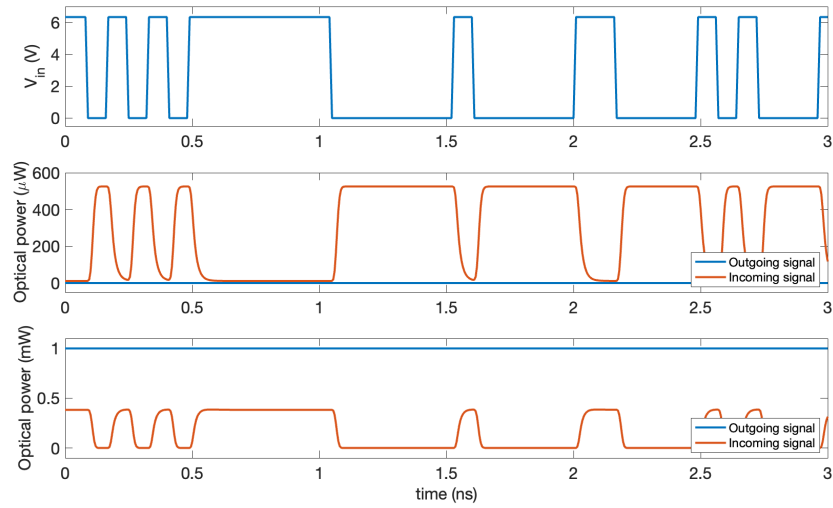


Fig. 4. Transient analysis results of the MIM. The top figure shows the modulating signal applied to the carrier depletion phase shifter. The middle and bottom figures illustrate the incoming and outgoing signals at the photodetector and laser, respectively.

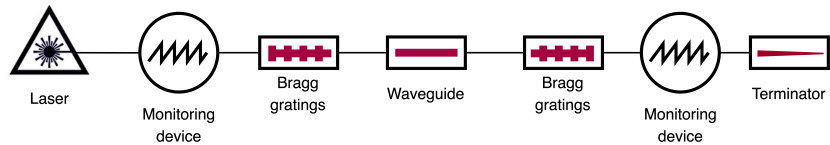


Fig. 5. Schematic diagram of the Bragg gratings based Fabry-Perot Cavity.

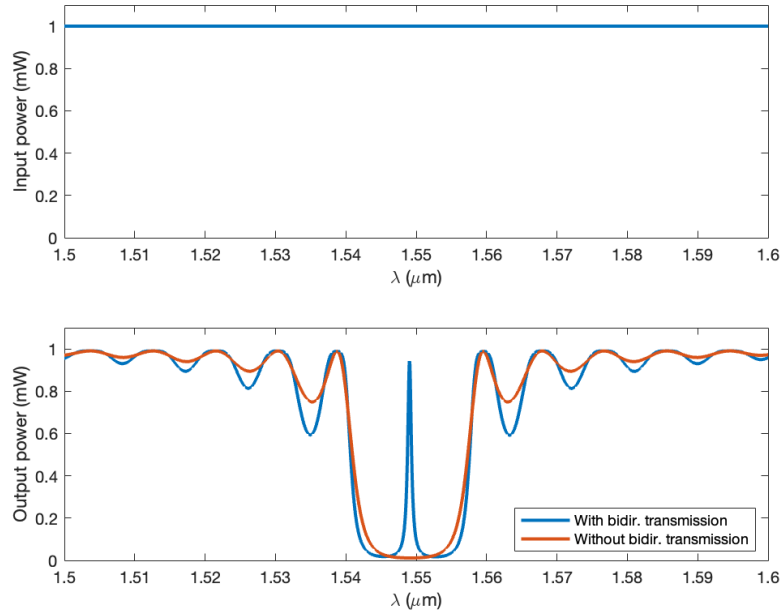


Fig. 6. Bandpass response of the Fabry-Perot cavity.

Since FPC is a circuit consisting of passive elements only, its baseband time domain response is static. Therefore the main focus is on its frequency spectrum. We run wavelength sweep simulation on the presented circuit to arrive at Fig. 6. According to the figure, the difference between the bidirectionality enabled simulation and conventional simulation is apparent. The latter fails to capture the bandpass behaviour at around 1549 nm, which may be critical for some applications. In this way, the proposed Verilog-A modeling fully captures the true FPC response, in contrast to the limitation described in [15]. Together, the two examples present a convincing case for Verilog-A modeling of silicon photonic devices.

#### 4. Conclusion

We have presented an approach to model photonic devices in Verilog-A. It handles forward and backward propagating signals in a single wire, removing the redundancy of the prior arts. Unlike prior art [8], it also supports multiple optical sources. Furthermore, our method enables integration of simulation and measurement data into Verilog-A models through s-parameters. In this way, one can capture response of any arbitrary passive photonic components. The simulation results showed the efficacy of our solution thereby making electro-optic co-simulation more convenient and accurate.

**Funding.** This work was supported in part by the Natural Sciences and Engineering Research Council of Canada and in part by Schmidt Sciences.

**Acknowledgements.** The authors would like to thank CMC Microsystems and Roozbeh Mehrabadi for access to CAD tools and technology.

**Disclosures.** The authors declare no conflicts of interest.

## References

1. S. Shekhar, W. Bogaerts, L. Chrostowski, J. E. Bowers, M. Hochberg, R. Soref, and B. J. Shastri, "Roadmapping the next generation of silicon photonics," *Nat. Commun.* **15** (2024).
2. J. Pond, G. S. Lamant, and R. Goldman, "Chapter 5 - Software tools for integrated photonics," in *Optical Fiber Telecommunications VII*, A. E. Willner, ed. (Academic Press, 2020), pp. 195–231.
3. E. Kononov, "Modeling photonic links in Verilog-A," Ph.D. thesis, Massachusetts Institute of Technology (2013).
4. C. Sorace-Agaskar, J. Leu, M. R. Watts, and V. Stojanovic, "Electro-optical co-simulation for integrated CMOS photonic circuits with VerilogA," *Opt. Express* **23**, 27180–27203 (2015).
5. J. Leu, "Integrated Silicon Photonic Circuit Simulations," Ph.D. thesis, Massachusetts Institute of Technology (2018).
6. P. Martin, F. Gays, E. Grellier, A. Myko, and S. Menezo, "Modeling of silicon photonics devices with Verilog-A," in *2014 29th International Conference on Microelectronics Proceedings - MIEL 2014*, (2014), pp. 209–212.
7. B. Wang, "Modeling of Photonic Devices and Photonic Integrated Circuits for Optical Interconnect and RF Photonic Front-End Applications," Ph.D. thesis, Texas A & M University (2016).
8. E. de Foucauld, O. Rozeau, A. Myko, D. Fowler, L. Viro, and F. Gays, "Compact modeling of photonic devices in Verilog-A for integrated circuit design," *Solid-State Electron.* **200**, 108538 (2023).
9. N. Schunk and K. Petermann, "Numerical analysis of the feedback regimes for a single-mode semiconductor laser with external feedback," *IEEE J. Quantum Electron.* **24**, 1242–1247 (1988).
10. H. Shoman, N. A. F. Jaeger, C. Mosquera, H. Jayatilleka, M. Ma, H. Rong, S. Shekhar, and L. Chrostowski, "Stable and Reduced-Linewidth Laser Through Active Cancellation of Reflections Without a Magneto-Optic Isolator," *J. Light. Technol.* **39**, 6215–6230 (2021).
11. C. R. Doerr, L. Chen, and D. Vermeulen, "Silicon photonics broadband modulation-based isolator," *Opt. Express* **22**, 4493–4498 (2014).
12. P. Dong, "Travelling-wave Mach-Zehnder modulators functioning as optical isolators," *Opt. Express* **23**, 10498–10505 (2015).
13. J. Hauck, M. Schrammen, S. Romero-García, J. Müller, B. Shen, J. Richter, F. Merget, and J. Witzens, "Stabilization and Frequency Control of a DFB Laser With a Tunable Optical Reflector Integrated in a Silicon Photonics PIC," *J. Light. Technol.* **34**, 5467–5473 (2016).
14. N. M. Kondratiev, V. E. Lobanov, A. E. Shitikov, R. R. Galiev, D. A. Chermoshentsev, N. Y. Dmitriev, A. N. Danilin, E. A. Lonshakov, K. N. Min'kov, D. M. Sokol, S. J. Cordette, Y.-H. Luo, W. Liang, J. Liu, and I. A. Bilenko, "Recent advances in laser self-injection locking to high-Q microresonators," *Front. Phys.* **18**, 21305 (2023).
15. J. K. Patel, E. Ghillino, and T. Korthorst, "Are Electrical Circuit Languages Robust Enough for Photonics?" <https://www.synopsys.com/content/dam/synopsys/photonic-solutions/documents/whitepapers/electro-optics-co-design.pdf>.
16. J. F. Pond, Z. Lu, A. R. Reid, V. Pacradouni, and J. F. Chung, "System and method for creating a single port interface for simulating bidirectional signals in circuits using available circuit simulation standards," (2020).
17. D. Pozar, *Microwave Engineering, 4th Edition* (Wiley, 2011).
18. Designer's Guide Consulting Inc., "Natures and Disciplines," <https://verilogams.com/refman/basics/disciplines.html>.
19. E. Säckinger, *Broadband Circuits for Optical Fiber Communication* (Wiley, 2005).
20. L. Chrostowski, Z. Lu, J. Flueckiger, X. Wang, J. Klein, A. Liu, J. Jhoja, and J. Pond, "Design and simulation of silicon photonic schematics and layouts," in *Silicon Photonics and Photonic Integrated Circuits V*, vol. 9891 L. Vivien, L. Pavesi, and S. Pelli, eds., International Society for Optics and Photonics (SPIE, 2016), p. 989114.
21. L. Chrostowski and M. Hochberg, *Silicon Photonics Design: From Devices to Systems* (Cambridge University Press, 2015).
22. Y. Zhang, S. Yang, Y. Yang, M. Gould, N. Ophir, A. E.-J. Lim, G.-Q. Lo, P. Magill, K. Bergman, T. Baehr-Jones, and M. Hochberg, "A high-responsivity photodetector absent metal-germanium direct contact," *Opt. Express* **22**, 11367–11375 (2014).